*Remote Sens.***2014**, *6*, 4723-4740; doi:10.3390/rs6064723

OPEN ACCESS

remote sensing

ISSN 2072-4292

www.mdpi.com/journal/remotesensing

Article

Developing Two Spectral Disease Indices for Detection of Wheat Leaf Rust (*Pucciniatriticina*)

Davoud Ashourloo [1,*], Mohammad Reza Mobasheri [1,*] and Alfredo Huete [2]

[1] Remote Sensing Group, Faculty of Geodesy and Geomatics Engineering, K.N. Toosi University of Technology, Tehran 19697-15433, Iran

[2] Plant Functional Biology and Climate Change Cluster, University of Technology Sydney, Ultimo, NSW 2007, Australia; E-Mail: Alfredo.Huete@uts.edu.au

***** Author to whom correspondence should be addressed; E-Mails: D_ashourloo@sbu.ac.ir (D.A.), Mobasheri@kntu.ac.ir (M.R.M.); Tel.: +98-21-2990-3077; Fax: +98-21-2243-1788.

Received: 24 February 2014; in revised form: 23 April 2014 / Accepted: 4 May 2014 / Published: 26 May 2014

Abstract: Spectral vegetation indices (SVIs) have been widely used to detect different plant diseases. Wheat leaf rust manifests itself as an early symptom with the leaves turning yellow and orange. The sign of advancing disease is the leaf colour changing to brown while the final symptom is when the leaf becomes dry. The goal of this work is to develop spectral disease indices for the detection of leaf rust. The reflectance spectra of the wheat's infected and non-infected leaves at different disease stages were collected using a spectroradiometer. As ground truth, the ratio of the disease-affected area to the total leaf area and the fractions of the different symptoms were extracted using an RGB digital camera. Fractions of the various disease symptoms extracted by the digital camera and the measured reflectance spectra of the infected leaves were used as input to the spectral mixture analysis (SMA). Then, the spectral reflectance of the different disease symptoms were estimated using SMA and the least squares method. The reflectance of different disease symptoms in the 450~1000 nm were studied carefully using the Fisher function. Two spectral disease indices were developed based on the reflectance at the 605, 695 and 455 nm wavelengths. In both indices, the R^2 between the estimated and the observed was as highas 0.94.

Keywords: wheat leaf rust; hyperspectral measurement; spectral disease indices; disease symptoms

---

1. Introduction

Various spectroscopic and imaging techniques have been developed to detect disease and stress in plants and trees [1].Spectral data at different scales including leaf, canopy and landscape-level have been widely used to improve precision [2–5]. In recent years, researchers have studied various spectral vegetation indices (SVIs) to detect different vegetation diseases [5–7]. Efficient use of spectral data in detection of plant disease depends on the application. The spectral regions from 400 to 700 and 700 to 1100 are mainly influenced by leaf composition of pigments, structure, and water content [8].

The effect of a disease on the pigments and structure of a plant and the change in their spectral responses enable spectroradiometry and remote sensing techniques to detect plant disease effectively [9].

There are indices derived from reflectance values at several wavelengths that are able to detect and quantify the leaf content substances such as chlorophyll, anthocyanin, and water[10,11]. Nalta *et al.* used leaf spectral reflectance to detect viral infection. In this study SVIs were used to identify infected and non infected leaves with maximum accuracy of 70% [12]. Chen *et al.* used hyperspectral measurement to identify cotton infected by verticillium wilt. The first derivatives between 731 and 1317 nm were the most effective in predicting disease [13]. Mohammad *et al.* showed that the visible and infrared regions of the electromagnetic spectra provide the maximum information on physiological stress levels in an affected plant [14]. Some of the wavelengths specific to a disease can be used to detect plant disease [15].Optimum spectral ranges have been suggested to detect different disease; 425, 685 and 735 nm to detect citrus canker [16], 737–925 nm to detect brown plant hopper disease of rice [17], 426 nm for brown plant hopper and leaf folder infestation of rice [18], and 800 to 1100 nm to identify leaf miner damage of tomato [19].

However, each disease may affect the leaf reflectance spectrum in a specific way. Therefore, special spectral disease indices (SDIs) must be developed to detect plant disease [8].In the SDIs and SVIs developed thusfar, less attention has been paid to the effect of disease symptoms on the reflectance spectra. It is therefore beneficial to design specific indices for each disease based on the progression of disease symptoms.

Wheat (*Triticumdicoccum*) has three types of rust disease called yellow rust, leaf rust, and stem rust. Leaf rust disease has the highest frequency of occurrence compared to the other two types, giving it higher priority for further investigations. Each year, this disease damages crops all around the world, decreasing yield dramatically. Leaf rust is caused by the *Pucciniatriticina* fungus and consists of different symptoms [20]. These symptoms begin by manifesting themselves in yellow, orange, and then dark brown colours. The final symptom is dry leaf. It is worth noting that the different symptoms of leaf rust can be simultaneously observed in various parts of a leaf [21].A few investigations have shown the potential of SVIs for disease detection. Mahlein *et al.* and Rump *et al.* demonstrated the effect of disease symptoms on recorded reflectance spectra [22–24].

In many investigations SVIs are deployed to study wheat rust in the leaf and canopy scales. In 1991, Hansen studied the effect of yellow rust on crop yield. Results show that hyperspectral data have the potential to detect changes in crop productivity due to rust disease with an R^2 of better than 0.9 [25]. In another study in 2007, Wenjiangn *et al.* investigated the relationship between wheat yellow rust and the photochemical reflectance index (PRI). This index was found to detect yellow colour variations

with an R^2 of better than 0.9 [26]. Regarding the fact that the effect of the deficiency of nitrogen is similar, the detection of wheat yellow rust *in situ*ations of nitrogen deficiency was studied by Zhang *et al.* using hyperspectral data. Results showed that wheat yellow rust can be detected when nitrogen is lacking [5].

Yellow rust is seen as narrow yellow strips parallel to nervures on the leaf whereas leaf rust appears as areas with various colours and patterns [15]. However, the number of studies on leaf brown rust is limited compared to yellow rust.

Devades *et al.* used 10 SVIs in the visible and near-infrared region to detect different types of rust at the leaf scale. In this study, none of these indices were able to detect and discriminate the three types of rust. However, the anthocyanin reflectance index (ARI) can be used to detect yellow rust, and the transformed chlorophyll absorption and reflectance index (TCARI) can be used to detect leaf rust [27]. In another studyconducted by Frank and Menz, hyperspectral and leaf multispectral data were used to estimate the severity of wheat leaf rust [28]. Results indicated that leaf rust could be detected in the early symptoms by using hyperspectral data. The algorithm used in this research was based on the minimum noise fraction (MNF) transformation. The reflectance spectra of the infected, non-infected, and dry area, as well as the soil class were taken at the canopy level. Although this research had acceptable results, it did not take into account the various disease symptoms.

Ashourloo *et al.* showed that the disease symptoms have a high impact on the infected plant reflectance spectra [29]. This means that as the disease severity increases, so does the collected spectrum variations at a specific disease severity. All of the SVI values were sensitive to disease severity so that the classification accuracy decreased as the disease severity increased. Results showed that as the disease severity increases, the scattering of the numerical values for all of the indices also increases. For the different SVIs, the amounts of scattering and classification accuracy are not the same and depend on the wavelength(s) used. It is necessary to develop SDIs for wheat leaf rust detection.

Wheat leaf rust at the leaf scale was studied for two purposes: (a) to estimate the reflectance spectra of various disease symptoms; and (b) to introduce an index for precise determination of disease severity using the spectral reflectance comparison of five different leaf colour symptoms.

2. Materials and Methods

2.1. Experimental Setup

A two-month campaign for collection of leaf reflectance data using a spectroradiometer was conducted. Also, a series of RGB digital photos from all infected leaves were collected. These data were used to develop indices in the visible and infrared ranges for detecting wheat leaf rust. Spectra were collected in controlled environmental conditions. In order to gather enough samples, wheat cultivation was repeated twice in consistently similar conditions. The purpose of this research was to develop an index (or indices) to accurately estimate disease severity, theleaf rust disease severity index (LRDSI). Here, the disease severity is defined as the fraction of the infected area. Also, an attempt was made to quantify the disease areas using the spectral response of the leaf. The flowchart for extracting the index is displayed in Figure 1.

Figure 1. Flowchart for extraction of wheat leaf rust disease.

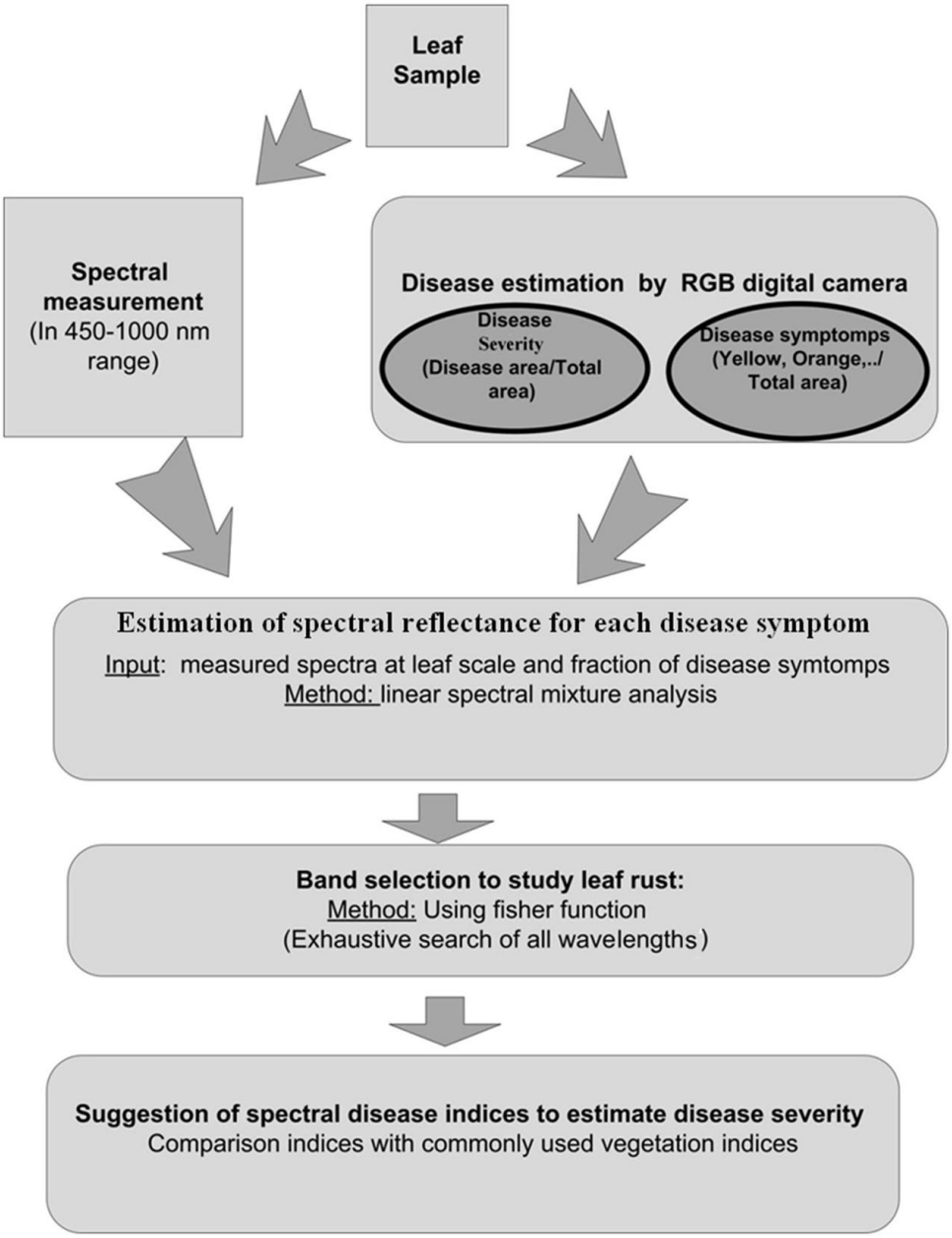

2.1.1. Cultivation Condition and Pathogen Inoculation

In order to conduct the experiment, the two most common cultivars of wheat called Bolani and Roshan were selected. Two cultivars were chosen so as to have a robust model with independent results to detect wheat leaf rust. These two types are sensitive to the leaf rust disease and are extensively planted in Iran. Cultivation was done in 1 by 1 m boxes in the Plant Protection Center of Iran. Both cultivars were grown in a greenhouse with temperature staying between 15 and 20 ℃, relative moisture more than 60%, and photoperiod of 16 hours a day. Spore suspension was sprayed on the plants—both front and back parts—from a 15 cm distance. Inoculation was performed at specific conditions (spore suspension 0.6 mL per plant at concentration of ~6 × 10^5 spores/mL, temperature 15–16 ℃, relative moisture more than 90%). Infected plants were transferred to a greenhouse with a temperature of 20–30 ℃, relative moisture of 90%, and with photoperiod of 16 hours a day. Each

time, the cultivation was conducted in 14 boxes: 7 boxes for the Bolani and 7 for the Roshan. The seeds were planted 5 cm apart. Watering and fertilizing were done in a controlled manner according to the needs of the plant. For each wheat item, 4 boxes were infected by spores and 3 boxes were kept as non-infected samples.

2.1.2. Data Collection

In order to measure spectral reflectance of the rust infected leaves, a spectroradiometer (Analytical Spectral Device, Boulder, CO, USA) with a 25° field of view was used. The spectra were collected in the 350–2500 nm range with a bandwidth of 1 to 4 nm. The Spectralon plate (Labsphere, Halma Co., USA) with a dimension of 40 × 40 cm was used as a reference. A contact probe (with leaf holder) was employed to reduce the effect of environmental light scattering and to improve the measurement accuracy. The distance from the probe inside contact probe to the target was 5.2 cm. Each of the leaves contained various disease symptom areas ranging from yellow to dark brown. Spectral sampling was performed from the initial symptom of the disease until the symptom of full infection (from 6 days after inoculation to 42 days). The reflectance spectrum sampling number was 5 where the average of these was used as the reflectance spectrum. After measuring the spectrum of each infected area, an RGB digital photo was taken. Each infected leaf was used only once for measurement. To avoid the absorption bands of water in wavelengths beyond 1000 nm, the electromagnetic region of 450 to 1000 nm was used in this work. In this operation, the infected leaves were separated and the measurement was carried out by placing the leaves on a flat surface where the contact probe was placed on the leaf. A total of 300 spectral samples were collected from the leaves with various disease symptoms areas. These data from infected and non-infected leaves were recorded on a weekly basis until 42 days after inoculation.

To determine the ratio and symptoms of the leaf rust disease, an RGB digital camera with the following specifications was used:

- Camera model: Canon DIGITAL IXUS 85 IS;
- F-109 number: f/3.2;
- Shutter speed: 1/60.

For all samples, the camera was held at the height of 30 cm above the samples.

Various symptoms of the leaf rust disease, including yellow, orange, dark brown and dry leaf, were extracted from the digital photos [21]. Different symptoms of wheat rust have been illustrated in Figure 2A,B. After spectrometry, photography was performed outdoors. Therefore, in order to remove the effect of the light intensity, the HIS system was used instead of the RGB system [30]. This algorithm is based on the transformation from the RGB to HIS space aiming to remove the effect of outdoor light intensity variations. Meanwhile, in this research, texture recognition algorithms were used to determine the boundaries of infected areas. The steps of classifying the disease symptoms by the images of the RGB digital camera are shown in Figure 2C. The amounts of different symptoms of the disease were determined by calculating the ratio of the areas of the infected spots to the total leaf area for each infected leaf. It must be taken into account that these measurements were conducted in the same area upon which the spectrometry had been performed. The exact location of the spectral

reflectance region on the leaf was marked with the contact probe so that the ratio and symptom of the disease could be extracted by the RGB digital camera. This area is displayed by a white circle in Figure 2D. Inside the marked area, a green mask was applied using a threshold value. The aim was to classify infected areas of the leaf with more precision. In addition, training samples were collected from the disease symptoms. Then, the maximum likelihood classification was applied on the H and S components in order to extract disease symptoms as shown in Figure 2C. The disease symptom fractions were used along with the spectra of the infected leaf as ground truth to evaluate the SVIs.

Figure 2. (**A**) Disease progress of wheat leaf rust; (**B**) Different symptoms of wheat leaf rust; (**C**) Classification steps of disease symptoms of wheat leaf rust by RGB digital camera; (**D**) Classification of different symptoms and masking green area of wheat leaf rust, the leaf area (fleaves were placed next to each other) marked by the contact probe is shown by the white circle.

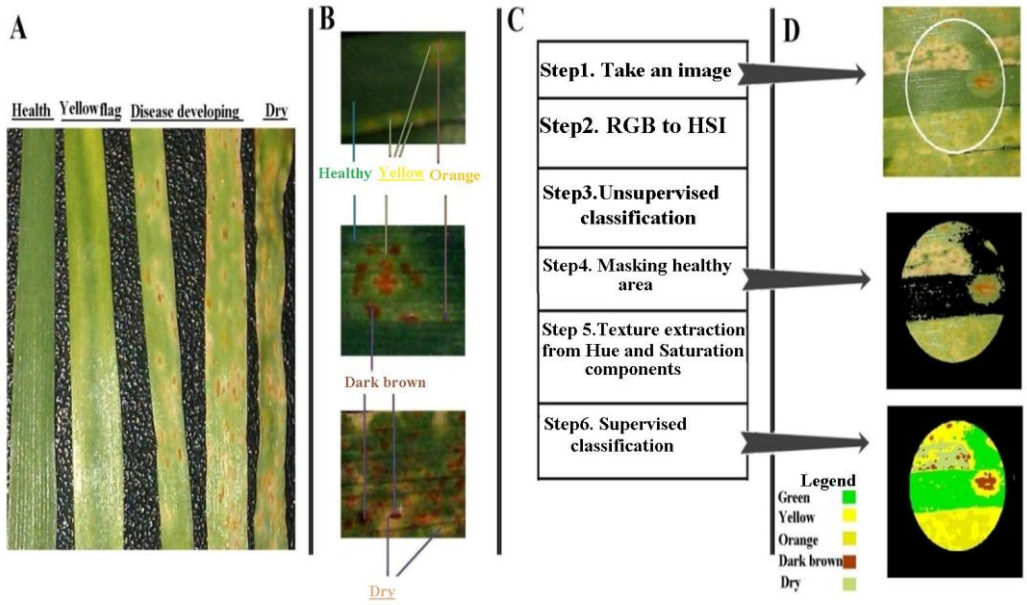

2.2. Extraction of Disease Reflectance Spectra

The results showed that the disease symptoms have high impact on the infected plant spectra [29]. It means that as the disease severity increases, so do the collected spectrum variations at a specific disease severity. It is expected that, for a specific disease, as the number of disease symptoms increases, the spectra will become more mixed at a specific disease severity level. SVIs are based on few spectral of vegetation. It was demonstrated, as the disease severity increases, so does the scattering of all SVI values. The scattering is caused by changes in disease symptom proportions from a point to another one for the same disease severity level. As a concluding remark, it was mentioned that the spectral mixture analysis of disease symptoms reduces the accuracy of SVIs [29].

The aim of this research is to develop SDIs to detect wheat leaf rust based on spectra of different disease symptoms. As Figure 2D shows, the spectra of infected leaves, recorded by the contact probe, are mixed. Therefore, this research tries to estimate the pure spectra of different disease symptoms by using spectral mixture analysis.

In remote sensing, the linear spectral mixing equations (LSME) are normally used in estimation of endmember abundance in each pixel. The method can be applied to mixed pixels and can be used for extraction of information at sub pixel scale. However, in this work, the fractions of each symptom area are known, and their corresponding reflectance spectra can thus be calculated.

In a rust disease infected leaf, one can find different symptoms such as green (healthy), yellow, orange, brown and dry areas with varying sizes. When the fraction of the areas of each symptom is known, then their reflectance values can be calculated by the following equation [31,32].

$$\rho'_{(k\lambda)} = \sum_{i=1}^{N} f_i \rho_{i\lambda} + \varepsilon_{k\lambda} \tag{1}$$

where ρ_λ is the reflectance measured by spectroradiometer, $\rho_{i\lambda}$ is the reflectance of disease symptoms area for sample *i* (*i* can be assumed as each sample recorded by the spectroradiometer and *k* is the number of sample) for a specific wavelength λ, f_i is the fraction of symptoms area of sample *i*, *N* is number of symptoms areas and ε_λ is the residual error. Sum of the fractions of all disease symptoms area is equal to 1. Equation (1) for k leaf spectral sample (recorded by spectroradiometer) in *N* class (*N* disease symptoms) can be written as Equation (2) below.

$$\begin{cases} \rho'_{(1\lambda)} = f_{(11)} \times \rho_{(\lambda 1)} + f_{(12)} \times \rho_{(\lambda 2)} + \ldots + f_{(1N)} \times \rho_{(\lambda N)} + \varepsilon_{(1\lambda)} \\ \rho'_{(2\lambda)} = f_{(21)} \times \rho_{(\lambda 1)} + f_{(22)} \times \rho_{(\lambda 2)} + \ldots + f_{(2N)} \times \rho_{(\lambda N)} + \varepsilon_{(2\lambda)} \\ \cdot \quad \cdot \quad \cdot \quad \cdot \quad \cdot \\ \rho'_{(k\lambda)} = f_{(k1)} \times \rho_{(\lambda 1)} + f_{(k2)} \times \rho_{(\lambda 2)} + \ldots + f_{(kN)} \times \rho_{(\lambda N)} + \varepsilon_{(k\lambda)} \end{cases} \tag{2}$$

The matrix form of the above equation system is as follows (by ignoring the residual part):

$$\rho' = F\rho \tag{3}$$

where:

$$\rho' = \begin{bmatrix} \rho'_{(1\lambda)} \\ \rho'_{(2\lambda)} \\ \cdot \\ \cdot \\ \cdot \\ \rho'_{(k\lambda)} \end{bmatrix} \quad F = \begin{pmatrix} f_{11} & f_{12} & \ldots & f_{1N} \\ f_{21} & f_{22} & \ldots & f_{2N} \\ \cdot & \cdot & \cdot & \\ \cdot & \cdot & \cdot & \\ \cdot & \cdot & \cdot & \\ f_{k1} & f_{k2} & & f_{kN} \end{pmatrix} \quad \rho = \begin{bmatrix} \rho_{(1\lambda)} \\ \rho_{(2\lambda)} \\ \cdot \\ \cdot \\ \cdot \\ \rho_{(N\lambda)} \end{bmatrix}$$

By solving Equation (3) through the least squares method (Equation (4)) for matrix ρ the reflectance of each symptom in one wavelength can be found. The procedure will be repeated over until we can find the reflectance curve for each symptoms area in all desired wavelengths.

$$\rho = (F^t F)^{-1} F^t \rho' \tag{4}$$

The final output is the spectral reflectance curves of disease for healthy leaf and four other different symptoms (colours). Output is a 5×55 matrix in which each row is the reflectance of one symptom of the disease in the 450–1000 nm electromagnetic range at 10 nm intervals. These extracted spectra of

disease symptoms have been shown in Figure 3 and is used in the next steps for the selection of appropriate wavelengths to build up desired indices.

Figure 3. Estimated reflectance spectra of healthy leaf and all other disease symptoms of wheat leaf rust.

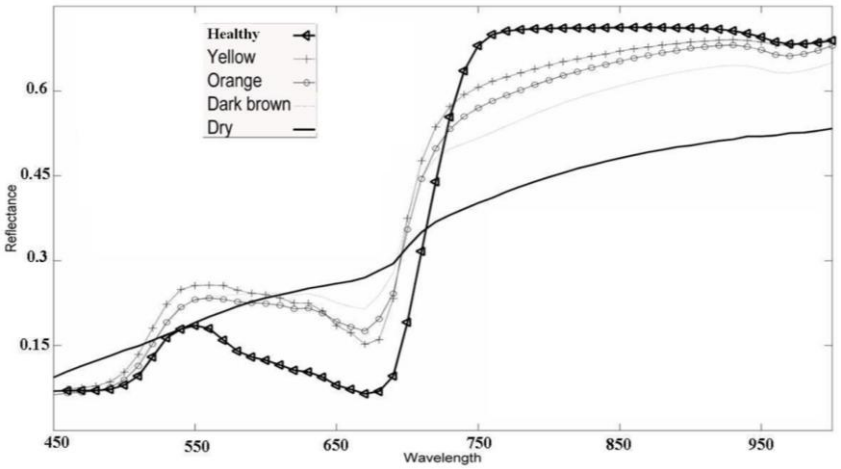

As can be seen in Figure 3, the spectra of different disease symptoms vary greatly in the 450–1000 nm range. There is little distinction in the blue and green regions while between red and red-edge regions the differences increase. The changes in reflectance of disease symptoms are not the same in the red-edge region where the green and dry areas have the maximum and minimum amount of variation, respectively. In the 800–950 nm range, the distinctions are more prominent and the reflectance decreases as the disease develops. The difference in the reflectance of disease symptoms at various wavelengths provides us with the possibility of selecting appropriate wavelengths for disease symptom determination.

2.3. Selection of Suitable Wavelength for Disease Severity Index

The symptoms of leaf rust appear at the end of the first week of inoculation as yellow in colour. As the disease develops, other symptoms/colours appear gradually. The goal is to determine the disease severity with high accuracy; in other words, it is desired to find the ratio of the infected area of the leaf, irrespective of the disease symptom. Then the areas of the infected and non-infected parts of the leaf are used to determine the disease severity. Remote sensing enables us to estimate these areas based on the differences between the reflectance of the healthy and the infected parts. The starker the differences are, the greaterthe ability of distinction will be. Interestingly, the area infected with leaf rust consists of different colours (symptoms). It is found that different disease symptoms have different spectra [24]. For a certain disease severity, disease symptoms may have different proportions. For example, if a leaf is 40%infected, in one situation, the fractions of the green, yellow, orange and brown areas will be 60%, 20%, 15% and 5%, respectively, while in another situation, these fractions are 60%, 10%, 10%, and 20%, respectively. Therefore, in the infected area, the fractions of the disease symptoms could encompass various situations. If in a specific wavelength, each symptom of the disease has a different reflectance from that of other symptoms, then different configurations will produce different spectra for a certain disease severity. Hence, the various reflectance spectra at a

certain disease severity may cause the scattering of the infected class to increase and, as a consequence, this scattering makes disease detection more difficult. To solve this problem, we must find a particular wavelength in which the reflectance values of different disease symptoms are the same, while these reflectance values are highly distinctive from the reflectance of the non-infected area. To find the suitable wavelength the Fisher function as stated in Equation (5) was used:

$$j(w) = \frac{(m_1 - m_2)^2}{S_1^2 + S_2^2} \quad (5)$$

This function is used to project a multidimensional space into a one-dimensional space. In the Fisher function, m and S are the class mean and variance, respectively. The indices1 and 2 represent the two classes studied in the function. The purpose of this function is to increase the difference between class means as well as simultaneously decreasing the difference between variances.

In this work, in order to select the appropriate wavelength, the reflectance spectra of four disease symptoms, as well as for healthy leaf were used as input in the Fisher function. The two classes used for analysis consist of the healthy and infected. The infected class consists of the reflectance of the yellow, orange, dark brown and red samples with the mean value of m_1 and variance value of S_1. The healthy class also consists of the green area with the mean value of m_2 and variance value of S_2. Because we only have one healthy sample, its variance is S_2 and m_2 is the reflectance of the green region at the wavelength being studied. The value of the Fisher function in the 450–1000 nm region was obtained based on the reflectance of disease symptoms in the form of healthy and infected classes. The wavelengths resulting in higher values of the Fisher function have better potential to estimate the disease severity.

2.4. Comparison of the Results with Other SVIs

SVIs have been used in a wide range of research activities for disease studies. SVIs are used to study the plant disease. Common SVIs were used to compare the results of disease studies. These indices include such spectral features as sensitivity to pigments, structural indices independent of pigments, chlorophyll absorption ratio index, narrow-band normalized vegetation index, nitrogen reflectance index, photochemical reflectance index, chlorophyll absorption and reflectance index, and anthocyanin reflectance index. More details are given in Table 1 [33–42]. Some of the indices such as PRI, TCARI and ARI have been used in wheat yellow rust studies.

Table 1. Spectral vegetation indices used for the comparison of results.

Variable	Definition	Description
NBNDVI	Narrow-band normalised difference vegetation index	$(R_{850} - R_{680})/(R_{850} + R_{680})$ [33]
NRI	Nitrogen reflectance index	$(R_{570} - R_{670})/(R_{570} + R_{670})$ [34]
PRI	Photochemical reflectance index	$(R_{570} - R_{531})/(R_{570} + R_{531})$ [35]
TCARI	The transformed chlorophyll absorption and reflectance Index	$3 \times [(R_{700} - R_{670}) - 0.2 \times (R_{700} - R_{550}) \times (R_{700}/R_{670})]$ [36]
SIPI	Structural independent pigment index	$(R_{800} - R_{445})/(R_{800} - R_{680})$ [37]
PhRI	Physiological reflectance index	$(R_{550} - R_{531})/(R_{550} + R_{531})$ [38]
NPCI	Normalized pigment chlorophyll ratio index	$(R_{680} - R_{430})/(R_{680} + R_{430})$ [39]

Table1.*Cont.*

Variable	Definition	Description
ARI	Anthocyanin reflectance index	$ARI = (R_{550})^{-1} - (R_{700})^{-1}$[40]
CARI	Chlorophyll absorption ratio index	$(\|(a670 + R_{670} + b)\|/(a^2 + 1)^{1/2}) \times (R_{700}/R_{670})$ $a = (R_{700} - R_{550})/150$, $b = R_{550} - (a \times 550)$ [40]
GI	Green index	R_{554}/R_{677}[41]
TVI	Triangular vegetation index	$0.5[120(R_{750} - R_{550}) - 200(R_{670} - R_{550})]$ [42]

3. Results and Discussions

3.1. Disease Development in Leaves Inoculated with Rust

For each infected leaf, the proportions of different disease symptoms including yellow, orange, brown, dry, and the disease severity (the sum of the proportions of different disease symptoms) for 7, 14, 21, 28, 35 and 42 days after inoculation were extracted with a digital camera. On each day, about 50 leaves were evaluated randomly and the average of the proportions of different disease symptoms and disease severity were estimated.

Figure 4 shows the proportions of different disease symptoms and disease severity for a 7-day interval until the 42nd day after inoculation. On the 7th day after inoculation, the proportion of the yellow area is low, but it reaches the maximum value on day 21 (37%). However, the proportion of the yellow area decreases a little after 21 days. The orange and dark brown areas appear on the 14th day after inoculation and show an increasing trend. They reach their maximum values on day 42. The proportions of the orange and dark brown areas on day 42 are 23% and 24% of the leaf area, respectively. The dry area appears 28 days after inoculation and reaches its maximum (18%) on the 42th day.As shown in the Figure 4, disease severity which is the sum of the proportions of different disease symptoms increases with time after inoculation and peaks on day 42.

Figure 4. Proportion ofdisease severity and different disease symptomsin wheat flag leaf infected by *Pucciniatriticina*fromday 7 to 42 after inoculation.

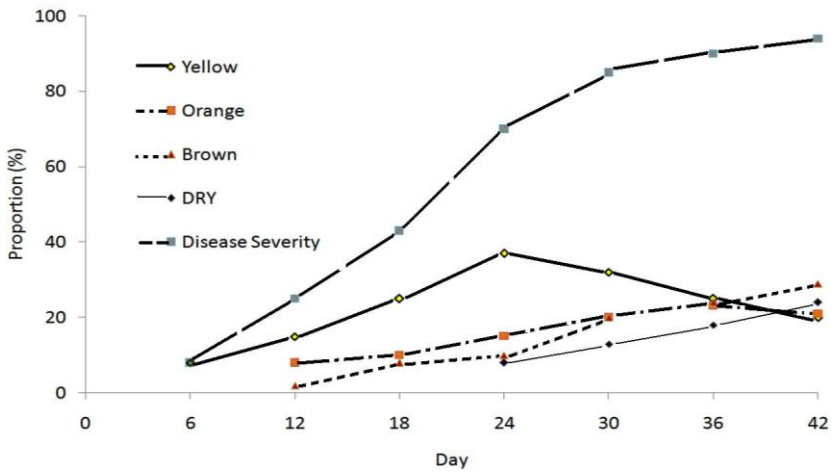

3.2. Evaluation of the Reflectance Spectra of Disease Symptoms

Due to the importance of disease severity estimation based on the analysis of the reflectance spectra of disease symptoms, it is necessaryto evaluate the accuracy of the spectra obtained for each disease symptoms. To this end, fraction values for each disease symptom were divided into ten equal ranges between 0 and 100. Equation (4) was then solved for the fractions, though this time the spectroradiometer measured reflectance and calculated symptoms reflectance values (Figure 3) were inputs to the equation. Subsequently, if the calculated spectra were extracted correctly, the calculated fractions of the disease symptoms must be equal to those estimated through the RGB digital camera. Therefore, the accuracy of the disease symptom spectra was evaluated through the following procedure:

(a) Selection of 60 random infected leaf spectra consisting of various disease symptoms
(b) Using the estimated spectra of disease symptoms (Figure 3) and calculating the fraction of each disease symptom in each leaf by deploying Equation (1). These values are called estimated values.
(c) Extracting the real fraction of disease symptoms for the selected spectra using the digital images. These values are called observed values.
(d) Calculating the correlation coefficient between the estimated and observed values.

The correlation coefficients obtained for the green, yellow, orange, brown, and dry area were 83%, 92%, 87%, 79%, and 88%, respectively. These results demonstrate that the extracted reflectance spectra are trustworthy.

3.3. Estimating the Disease Severity

The goal of the current research is to present a suitable index to estimate the disease severity. The Fisher function was used to select the appropriate wavelengths for disease severity estimation. The wavelength which is to be selected as the optimal one is extracted from the estimated spectra of disease symptoms shown in Figure 3.

According to Figure 5A, the Fisher function yields high values in the red and red-edge regions. The Fisher values obtained at the 605 and 695 nm wavelengths were high and had the values of 188 and 164, respectively (Figure 5A). As Figure 3 shows, not only the disease symptoms have the least amount of differences in reflectance, but they also have the highest difference with the reflectance of healthy parts of leaf at these wavelengths. For further assurance, the reflectance values of the healthy and infected areas were studied. According to Figure 3, the reflectance of the leaf at various stages of the disease at the 605 nm wavelength was similar and was about 0.26, while for the dry area, reflectance was a little higher and about 0.29. This difference reduces the accuracy of the index based on the 615 nm reflectance. To solve this problem, the ratio of the reflectance values at 605 to 455 nm was used; the index made by this ratio is the leaf rust disease severity index 1(LRDSI_1). At 455 nm wavelength, the reflectance of the healthy area and disease symptoms were similar at about 0.06, whereas in the dry area, the reflectance was a little higher. Hence, by dividing reflectance at 605 nm by reflectance at 455 nm, the difference of the values obtained for the dry and disease symptoms were minimized. Another region was at 695 nm. At this wavelength, the amount of reflectance for the healthy area is 0.15 and for the yellow, orange, and dark brown disease symptoms, 0.28, 0.28, and 0.29 (Figure 3). For the dry area, the reflectance is a little higher around 0.31. Again, if it is divided by the

reflectance at 455 nm, the difference between the dry area and disease symptoms will be minimized. The index made by this ratio is named the leaf rust disease severity index 2(LRDSI_2). In Figure 5B, the linear regression of the ratio of the reflectance in two wavelengths with the disease severity is given. The dry areas have higher R^2. As can be seen in Figure 5B, the ratios of the reflectance at 605 and 695 nm wavelengths to the reflectance at 455 nm wavelength have the highest values. This shows that the wavelengths used to estimate the disease severity have been properly selected. Furthermore, the disease symptoms and healthy areas have the highest amount of difference in reflectance as was the goal. In Figure 5C,D, the correlation between the proposed indices of LRDSI_1 and LRDSI_2 and the disease severity is presented. The correlation for both indices is as high as about 0.94. The estimation of the leaf disease severity based on the 605 and 695 nm wavelengths is given in Equations (7) and (8).

$$\text{Leaf Rust Disease Severity Index 1(LRDSI\_1)} = 6.9\ \frac{\rho_{605}}{\rho_{455}} - 1.2 \tag{7}$$

$$\text{Leaf Rust Disease Severity Index 2(LRDSI\_2)} = 4.2\ \frac{\rho_{695}}{\rho_{455}} - 0.38 \tag{8}$$

Figure 5. (**A**) Values of the Fisher function at various wavelengths used for disease severity estimation; (**B**) R^2 values between the reflectance ratio of two wavelengths and the leaf disease severity; (**C**) The correlation between the disease severity and ratio of reflectance at 605 nm and 455 nm; (**D**) The correlation between the disease severity and ratio of reflectance at 695 nm and 455 nm wavelengths.

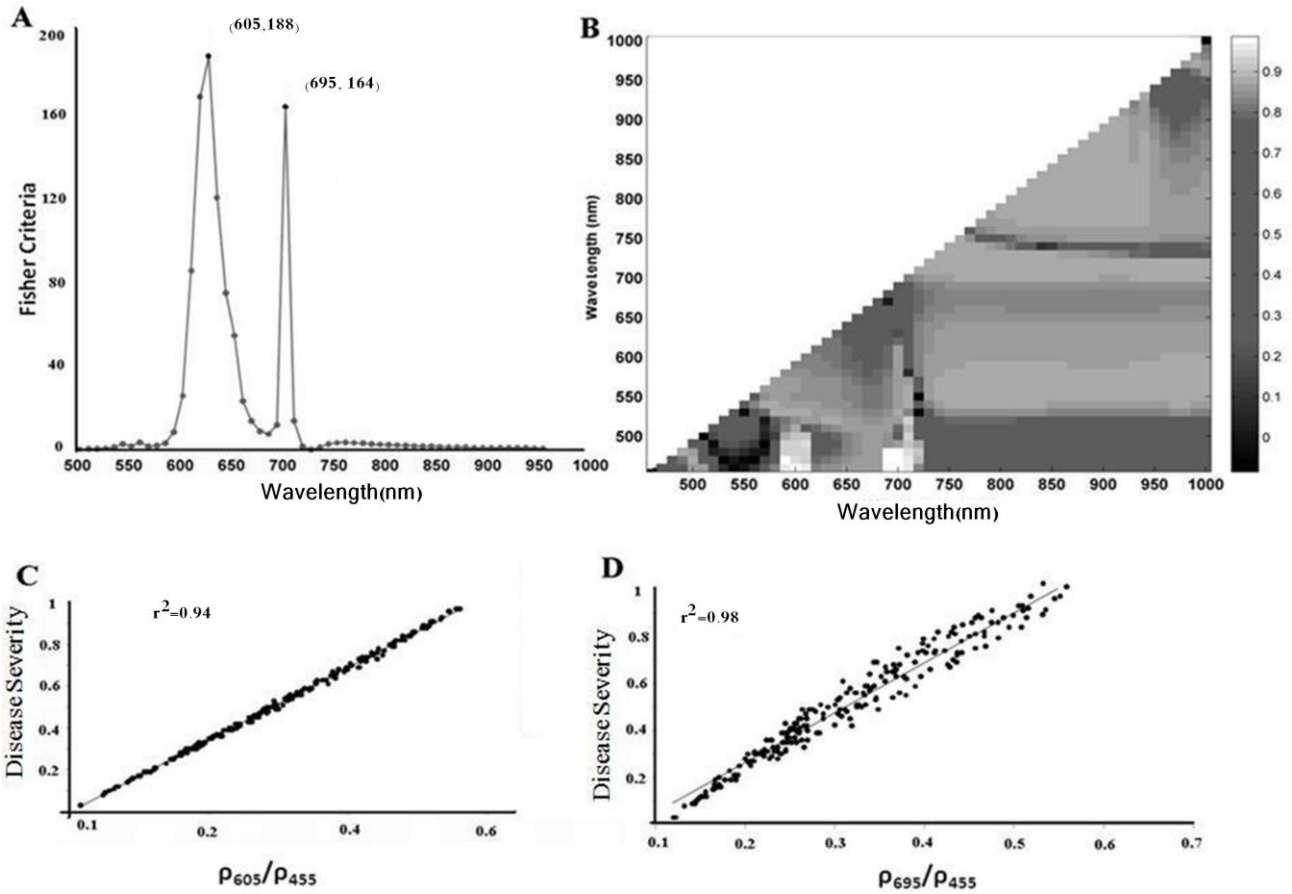

The evaluation of the proposed indices is given in Table 2. As the matrix shows for the two indices, the disease severity estimation using LRDSI_1 has an overall accuracy of 89.5%, and accuracies of 87% and 91% for the infected and non-infected areas, respectively. The disease severity estimation using LRDSI_2 has an overall accuracy of 86.5%, and accuracies of 87% and 86% for the infected and non-infected areas, respectively. Table 3 shows the classification error for the disease symptoms. At first, the classification error was high (1%–5%) and then increases slightly at higher values (5%–60%). Finally, it decreases again at higher values (60%–100%). Both indices have a classification error of less than 10% in the 20–100 range. This demonstrates the efficiency of the proposed indices to estimate the disease at ratios bigger than 5%.

Table 2. Classification accuracy for the healthy and infected classes using leaf rust disease severity indices.

Class Precision	Prediction	Ground Truth	Class Precision
$\boldsymbol{LRASI\_1_{\underline{\rho 605}}}$	Rust	Healthy	
Rust	140	20	87%
Healthy	11	127	91%
Class recall	93%	86%	89.5
$\boldsymbol{LRASI\_2_{\underline{\rho 605}}}$	Rust	Healthy	
Rust	148	22	87%
Healthy	21	135	86%
Class recall	87%	86%	86.5%

Table 3. Classification error for the healthy and infected classes using LRDSI index.

Disease Severity	Classification Error %			
	$\boldsymbol{LRASI\_1_{\underline{\rho 605}}}$		$\boldsymbol{LRASI\_2_{\underline{\rho 605}}}$	
	Rust	Healthy	Healthy	Rust
1%–5%	35	44	47.7	32
5%–10%	10.2	14.3	16	17.2
10%–20%	7.2	11.6	12.4	9.8
20%–30%	5.1	7.6	8.3	7.4
30%–40%	3.6	3.1	3.6	4.5
40%–50%	3.9	2.4	2.7	5
50%–60%	1.2	2.2	0.9	1.7
60%–70%	3	4.7	2.4	3.7
70%–80%	5.1	4.5	3.7	3.5
>80%	4.8	5	4.1	4.4

3.4. Comparison Suggested Indices with Other SVIs

Different coefficients of determination (R^2) are observed in the relationship between SVIs and disease severity. The R^2 values are shown in Figure 6. NBNDVI (Figure 6K) with the R^2 of 0.75, and MCRI (Figure 6E) with the R^2 of 0.34 have the strongest and weakest relation with the disease severity respectively.

Figure 6. The relation between spectral features and the disease severity (**A** to **K**).Changes of first derivative sums and the disease severity in the same direction (**L**).

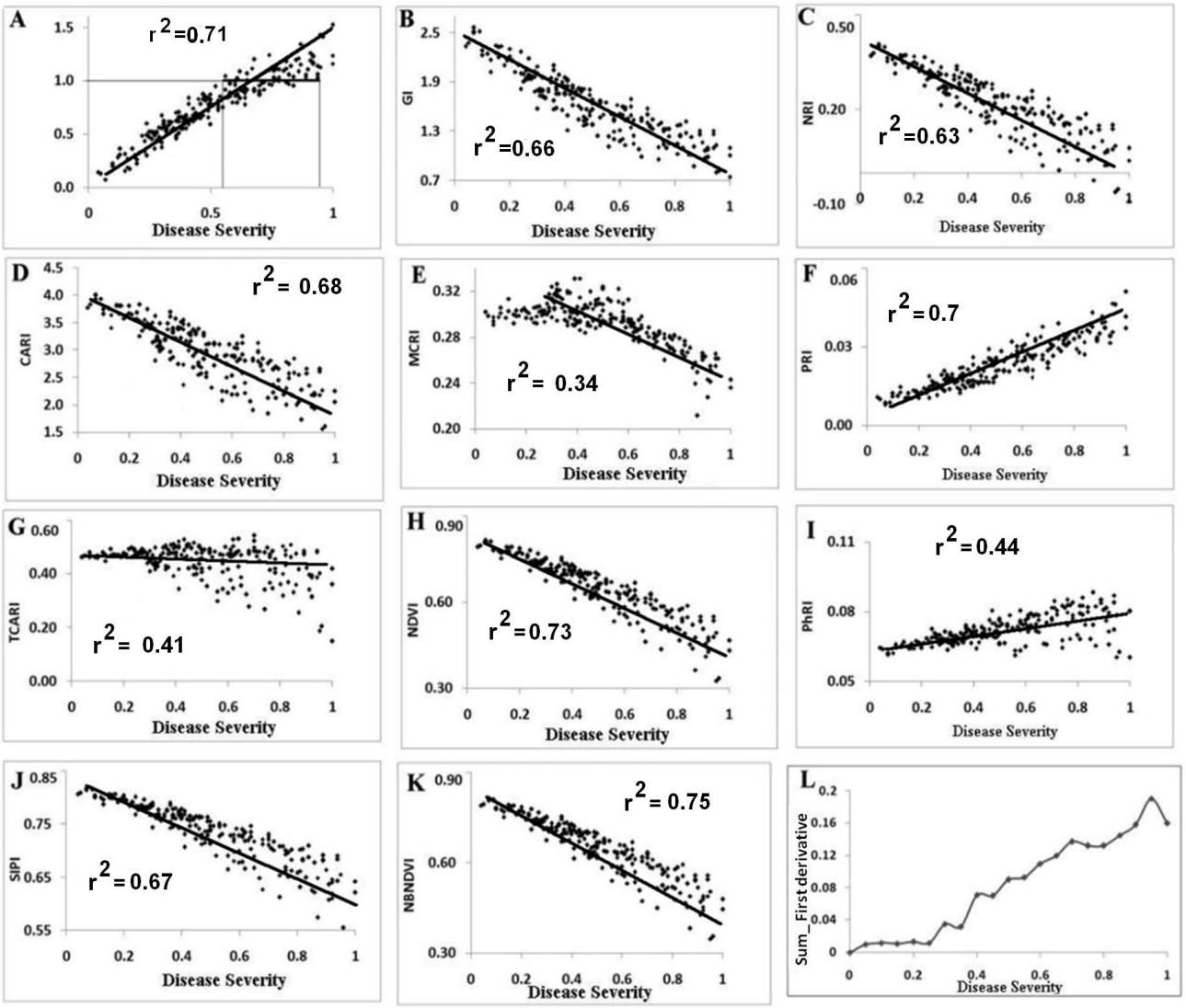

Although some indices such as NBNDVI, PRI, and NDVI have high R^2 with the disease severity, the data scatter increases as the disease severity increases. The increase in data scattering at higher ratios causes a decrease in the accuracy of disease severity estimation. As Table 4 shows, for NBNDVI, PRI, and NDVI, the highest accuracy is obtained for severity values between 5% and 40%. For severity values higher than 40%, the classification accuracy decreases so that values above 70% yield a minimum classification error of around 40%. For further investigation, the relation between reflectance variations and the disease severity was examined. The sum of the first derivatives of each spectrum in the 450–1000 nm range was used as the representative of the spectrum. As previously stated, for each measured spectrum, the disease severity was extracted using an RGB digital camera; therefore, it is possible to study spectral variations as a function of the disease severity. According to Figure 6L, the disease severity has a positive relation with the sum of the first derivatives. It can be said that at high disease severity, the disease symptoms have a great impact on the increase of spectral distinction and data scattering.

As Figure 5C,D show, the R^2 of LRDSI_1 and LRDSI_2 indices with the disease severity is larger than 0.9.These results are much better than those of PRI, NBNDVI, and NDVI.

Table 4. Classification accuracy for the healthy and infected classes for NDVI, PRI and NBNDVI.

Disease Severity	Classification Error %					
	NBNDVI		NDVI		PRI	
	Rust	Healthy	Healthy	Rust	Healthy	Rust
1%–5%	25	34	29	38	44	43
5%–10%	12	14	13	14	11	19
10%–20%	11	12	14	10	13	18
20%–30%	15	10	17	14	17	15
30%–40%	14	13	26	18	11	22
40%–50%	25	21	26	28	21	28
50%–60%	28	29	19	37	29	32
60%–70%	31	37	44	36	34	47
70%–80%	38	55	47	54	44	61
>80%	53	44	61	52	49	58

4. Conclusions

The results of this research showed that leaf rust has various symptoms with a distinct spectrum for each. The investigation carried out by the Fisher function into the spectra of the disease symptoms at the 450–1000 nm range revealed little distinction between the spectra at the red and red-edge regions. Furthermore, at these regions, there exists the greatest discrepancy between the reflectance spectra of the disease symptoms and those of the non-infected areas. Both of the proposed indices have high capability to estimate the leaf rust disease. However, disease estimation is faced with much difficulty at the onset of early symptoms due to the underdevelopment of the disease and the spectral similarity between the yellow and non-infected areas. The proposed indices better account for explain variations in disease progressing compared to other common SVIs. Based on this research, it was revealed that in the common SVIs, data scattering increases as the disease develops. The amount of scattering and correlation is not the same and depends on the wavelength(s) used. The proposed indices (LRDSI_1 and LRDSI_2) not only have high accuracy but also reduce data dimensionality and speed up the disease estimation rate. It must be noted that the proposed indices need to be tested on various sensors and different varieties of wheat in order to be used in precision farming. Also, suggested SDIs must be tested in different environments, scales, field conditions. Finally, it is highly essential to develop indices based on spectral variations for other types of vegetation diseases that have various symptoms.

Author Contributions

Ashourloo D. and Mobasheri M.R. developed the concept and research plan. Mobasheri was primary supervisor and leaded the campaign and field working. Huete A. co-supervisor of this work. Ashourloo, Mobasheri and Huete provided expert knowledge about methods, interpretations,

participated in the discussions, editing and revisions of the paper. All authors discussed the results and implications and commented on the manuscript at all stages.

Conflicts of Interest

The authors declare no conflict of interest.

References

1. Sankaran, S.; Mishra, A.; Ehsani, R.; Davis, C. A review of advanced techniques for detecting plant diseases. *Comput. Electron. Agric.* **2010**, *72*, 1–13.
2. Roelofsen, H.D.; van Bodegom, P.M.; Kooistra, L.; Witte, J.-P.M. Trait estimation in herbaceous plant assemblages from *in situ* canopy spectra. *Remote Sens.* **2013**, *5*, 6323–6345.
3. Delalieux, S.; Auwerkerken, A.; Verstraeten, V.W.; Somers, B.; Valcke, R.; Lhermitte, S.; Keulemanss, J.; Coppin, P. Hyperspectral reflectance and fluorescence imaging to detect scab induced stress in Apple leaves. *Remote Sens.* **2009**, *1*, 858–874.
4. Steiner, U.; Bürling, K.; Oerke, E.-C. Sensor use in plant protection. *Gesunde Pflanz.* **2008**, *60*, 131–141.
5. Zhang, J.; Pu, R.; Huang, W.; Yuan, L.; Luo, J.; Wang, J. Using *in-situ* hyperspectral data for detecting and discriminating yellow rust disease from nutrient stresses. *Field Crops Res.* **2012**, *134*, 165–174.
6. Hillnhütter, C.; Mahlein, A.-K.; Sikora, R.A.; Oerke, E.-C. Remote sensing to detect plant stress induced by *Heterodera schachtii* and *Rhizoctonia solani* in sugar beet fields. *Field Crops Res.* **2011**, *122*, 70–77.
7. Moshou, D.; Bravo, C.; West, J.; Wahlen, S.; McCartney, A.; Ramon, H. Automatic detection of "yellow rust" in wheat using reflectance measurements and neural networks. *Comput. Electron. Agric.* **2004**, *44*, 173–188.
8. Mahlein, A.-K.; Rumpf, T.; Welke, P.; Dehne, H.-W.; Plümer, L.; Steiner, U.; Oerke, E.-C. Development of spectral indices for detecting and identifying plant diseases. *Remote Sens. Environ.* **2013**, *128*, 21–30.
9. Zhang, J.-C.; Pu, R.-L.; Wang, J.-H.; Huang, W.-J.; Yuan, L.; Luo, J.-H. Detecting powdery mildew of winter wheat using leaf level hyperspectral measurements. *Comput. Electron. Agric.* **2012**, *85*, 13–23.
10. Gitelson, A.A.; Kaufman, Y.J.; Stark, R.; Rundquist, D. Novel algorithms for remote estimation of vegetation fraction. *Remote Sens. Environ.* **2002**, *80*, 76–87.
11. Peñuelas, J.; Baret, F.; Filella, I. Semiempirical indices to assess carotenoids/chlorophyll a ratio from leaf spectral reflectance. *Photosynthetica* **1995**, *31*, 221–230.
12. Naidu, R.A.; Perry, E.M.; Pierce, F.J.; Mekuria, T. The potential of spectral reflectance technique for the detection of Grapevine leaf roll-associated virus-3 in two red-berried wine grape cultivars. *Comput. Electron. Agric.* **2009**, *66*, 38–45.
13. Chen, B.; Wang, K.; Li, S.; Wang, J.; Bai, J.; Xiao, C.; Lai, J. Spectrum Characteristics of Cotton Canopy Infected with Verticillium Wilt and Inversion of Severity Level. In *IFIP International Federation for Information Processing*; Springer: Boston, MA, USA, 2008; pp. 1169–1180.

14. Muhammad, H.H. Using Hyperspectral Reflectance Data for Discrimination between Healthy and Diseased Plants, and Determination of Damage-level in Diseased Plants. In Proceedings of the 31st Applied Imagery Pattern Recognition Workshop, Washington, DC, USA, 16–18 October 2002; pp. 49–54.
15. West, J.S.; Bravo, C.; Oberti, R.; Lemaire, D.; Moshou, D.; McCartney, H.A. The potential of optical canopy measurement for targeted control of field crop disease. *Annu. Rev. Phytopathol.* **2003**, *41*, 593–614.
16. Belasque, L.; Gasparoto, M.C.G.; Marcassa, L.G. Detection of mechanical and disease stresses in citrus plants by fluorescence spectroscopy. *Appl. Opt.* **2008**, *47*, 1922–1926.
17. Yang, C.M.; Cheng, C.H. Spectral characteristics of rice plants infested by brown planthoppers. *Proc. Natl. Sci. Counc. Repub. China Part B Life Sci.* **2001**, *25*, 180–186.
18. Yang, C.M.; Cheng, C.H.; Chen, R.K. Changes in spectral characteristics of rice canopy infested with brown planthopper and leaffolder. *Crop. Sci.* **2007**, *47*, 329–335.
19. Xu, H.R.; Ying, Y.B.; Fu, X.P.; Zhu, S.P. Near-infrared spectroscopy in detecting leaf miner damage on tomato leaf. *Biosyst. Eng.* **2007**, *96*, 447–454.
20. Bolton, M.; Kolmer, J.; Garvin, D. Wheat leaf rust caused by Puccinia triticina. *Mol. Plant. Patol.* **2008**, *9*, 563–575.
21. Robert, C.; Bancal, M.-O.; Ney, B.; Lannou, C. Wheat leaf photosynthesis loss due to leaf rust, with respect to lesion development and leaf nitrogen status. *New Phytol.* **2005**, *165*, 227–241.
22. Mahlein, A.-K.; Steiner, U.; Dehne, H.-W.; Oerke, E.-C. Spectral signatures of sugar beet leaves for the detection and differentiation of diseases. *Precis. Agric.* **2010**, *11*, 413–431.
23. Rumpf, T.; Mahlein, A.-K.; Steiner, U.; Oerke, E.-C.; Dehne, H.-W.; Plümer, L. Early detection and classification of plant diseases with support vector machines based on hyperspectral reflectance. *Comput. Electron. Agric.* **2010**, *74*, 91–99.
24. Mahlein, A.-K.; Steiner, U.; Hillnhütter, C.; Dehne, H.-W.; Oerke, E.-C. Hyperspectral imaging for small-scale analysis of symptoms caused by different sugar beet diseases. *Plant. Methods*. **2012**, *8*, doi:10.1186/1746-4811-8-3.
25. Hansen, J.G. Use of multispectral radiometry in wheat yellow rust experiments. *OEPP/EPPO Bull.* **1991**, *21*, 651–658.
26. Huang, W.; Lamb, D.W.; Niu, Z.; Zhang, Y.; Liu, L.; Wang, J. Identification of yellow rust in wheat using *in-situ* spectral reflectance measurements and airborne hyperspectral imaging. *Precis. Agric.* **2007**, *8*, 187–119.
27. Devadas, R.; Lamb, D.W.; Simpfendorfer, S.; Backhouse, D. Evaluating ten spectral vegetation indices for identifying rust infection in individual wheat leaves. *Precis. Agric.* **2009**, *10*, 459–470.
28. Franke, J.; Menz, G. Multi-temporal wheat disease detection by multi-spectral remote sensing. *Precis. Agric.* **2007**, *8*, 161–172.
29. Ashourloo, D.; Mobasheri, M.R.; Huete, A. Evaluating the effect of different wheat rust disease symptoms on vegetation indices using hyperspectral measurements. *Remote Sens.* **2014**, in press.
30. Al-Hiary, H.; Bani-Ahmad, S.; Reyalat, M.; Braik, M.; ALRahamneh, Z. Fast and accurate detection and classification of plant diseases. *Int. J. Comput. Appl.* **2011**, *17*, 31–38.
31. Zurita-Milla, R.; Clevers, J.G.P.W.; Schaepman, M.E. Unmixing-based LANDSAT TM and MERIS FR data fusion. *IEEE Geosci. Remote Sens. Lett.* **2008**, *5*, 453–457.

32. Dennison, P.E.; Roberts, D.A. Endmember selection for multiple endmember spectral mixture analysis using endmember average RMSE. *Remote Sens. Environ.* **2003**, *87*, 123–135.
33. Thenkabail, P.S.; Smith, R.B.; de Pauw, E. Hyperspectral vegetation indices and their relationships with agricultural crop characteristics. *Remote Sens. Environ.* **2000**, *71*, 158–182.
34. Filella, I.; Serrano, L.; Serra, J.; Penuelas, J. Evaluating wheat nitrogen status with canopy reflectance indices and discriminant analysis. *Crop. Sci.* **1995**, *35*, 1400–1405.
35. Gamon, J.A.; Penuelas, J.; Field, C.B. A narrow-waveband spectral index that tracks diurnal changes in photosynthetic efficiency. *Remote Sens. Environ.* **1992**, *41*, 35–44.
36. Haboudane, D.; John, R.; Millera, J.R.; Tremblay, N.; Zarco-Tejada, P.J.; Dextraze, L. Integrated narrow-band vegetation indices for prediction of crop chlorophyll content for application to precision agriculture. *Remote Sens. Environ.* **2002**, *81*, 416–426.
37. Penuelas, J.; Gamon, J.A.; Fredeen, A.L.; Merino, J.; Field, C.B. Reflectance indices associated with physiological changes in nitrogen- and water-limited sunflower leaves. *Remote Sens. Environ.* **1995**, *48*, 135–146.
38. Gitelson, A.A.; Merzlyak, M.N.; Chivkunova, O.B. Optical properties and nondestructive estimation of anthocyanin content in plant leaves. *Photochem. Photobiol.* **2001**, *74*, 38–45.
39. Kim, M.S.; Daughtry, C.S.T.; Chappelle, E.W.; McMurtrey, J.E. The Use of High Spectral Resolution Bands for Estimating Absorbed Photosynthetically Active Radiation (APAR). In Proceedings of the 6th International Symposium on Physical Measurements and Signatures in Remote Sensing, Val d'Isère, France, 17–21 January 1994, pp. 299–306.
40. Zarco-Tejada, P.J.; Berjón, A.; López-Lozano, R.; Miller, J.R.; Martín, P.; Cachorro, V.; González, M.R.; Frutos, A. Assessing vineyard condition with hyperspectral indices: Leaf and canopy reflectance simulation in a row-structured discontinuous canopy. *Remote Sens. Environ.* **2005**, *99*, 271–287.
41. Broge, N.H.; Leblanc, E. Comparing prediction power and stability of broadband and hyperspectral vegetation indices for estimation of green leaf area index and canopy chlorophyll density. *Remote Sens. Environ.* **2000**, *76*, 156–172.
42. Haboudane, D.; Miller, J.R.; Pattery, E.; Zarco-Tejad, P.J.; Strachan, I.B. Hyperspectral vegetation indices and novel algorithms for predicting green LAI of crop canopies: Modeling and validation in the context of precision agriculture. *Remote Sens. Environ.* **2004**, *90*, 337–352.